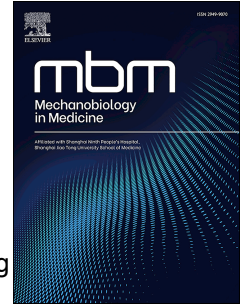


Journal Pre-proof

Overstretch causes lipid accumulation in vascular smooth muscle cells dependent on NADPH oxidase 1

Jiazhen Zhang, Qinfen Li, Suoqi Ding, Wei Xu, Jilei Su, Jingang Cui, Yongsheng Ding



PII: S2949-9070(25)00017-8

DOI: <https://doi.org/10.1016/j.mbm.2025.100129>

Reference: MBM 100129

To appear in: *Mechanobiology in Medicine*

Received Date: 20 December 2024

Revised Date: 27 February 2025

Accepted Date: 23 March 2025

Please cite this article as: J. Zhang, Q. Li, S. Ding, W. Xu, J. Su, J. Cui, Y. Ding, Overstretch causes lipid accumulation in vascular smooth muscle cells dependent on NADPH oxidase 1, *Mechanobiology in Medicine*, <https://doi.org/10.1016/j.mbm.2025.100129>.

This is a PDF file of an article that has undergone enhancements after acceptance, such as the addition of a cover page and metadata, and formatting for readability, but it is not yet the definitive version of record. This version will undergo additional copyediting, typesetting and review before it is published in its final form, but we are providing this version to give early visibility of the article. Please note that, during the production process, errors may be discovered which could affect the content, and all legal disclaimers that apply to the journal pertain.

© 2025 The Author(s). Published by Elsevier B.V. on behalf of Shanghai Ninth People's Hospital, Shanghai Jiao Tong University School of Medicine.

Overstretch causes lipid accumulation in vascular smooth muscle cells dependent on NADPH oxidase 1

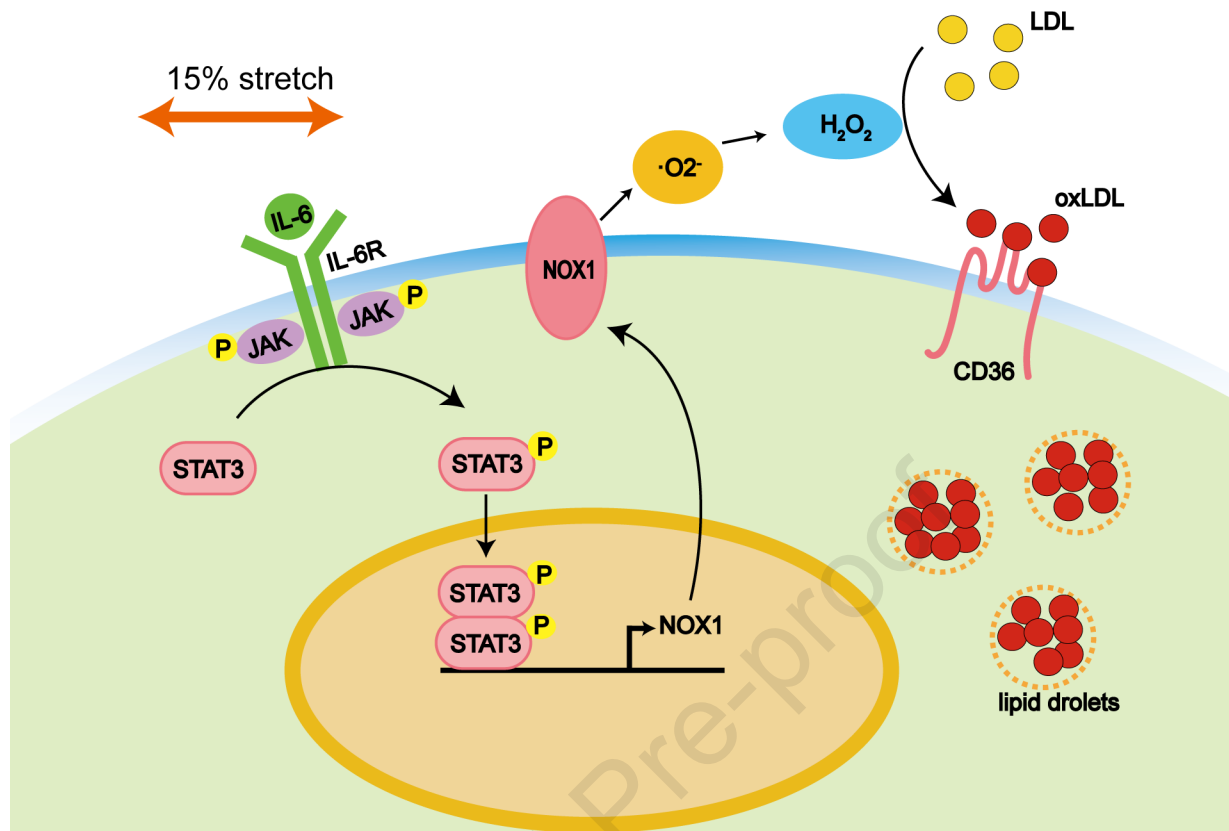
Jiazhen Zhang¹, Qinfen Li¹, Suoqi Ding², Wei Xu¹, Jilei Su¹, Jingang Cui¹, Yongsheng Ding^{1*}

¹College of Life Sciences, University of Chinese Academy of Sciences, Beijing 101408, China

²School of Chemistry, Beihang University, Beijing, 100191, China

*Corresponding author: Yongsheng Ding

Email: dingysh@ucas.edu.cn



Abstract

At the bend and bifurcation of arteries prone to atherosclerosis, pulsatile blood retention may cause overstretch on the tube wall. It has been reported that more than half of the foam cells found in atherosclerotic plaques are derived from vascular smooth muscle cells (VSMCs), but the mechanism is not adequately understood. In this work, we used a microfluidic device to apply a cyclic stretch (15% and 0.05 Hz) on the VSMC for 24 h. The stretch caused a significant increase in the intracellular lipid accumulation, accompanying with the increased NOX1 and CD36 protein expression. On the other hand, inhibition of NOX1 activity, elimination of reactive oxygen species (ROS), or knockdown of NOX1 expression could significantly inhibit intracellular lipid accumulation. In addition, the NOX1 upregulation caused by 15% stretch was related to the JAK/STAT signaling pathway. Our results reveal a novel mechanism of VSMC foam cell formation caused by the upregulation of NOX1.

Keywords: overstretch, NADPH oxidase 1, lipid accumulation, vascular smooth muscle cells, atherosclerosis

Introduction

Atherosclerosis is a chronic inflammatory disease characterized by lipid and fibrous components accumulation in arterial wall ¹. Typically, the formation of foam cells is thought to be the result of excessive oxidized low-density lipoprotein (ox-LDL) engulfed by monocytes that infiltrate the sub-endothelial layer. However, vascular smooth muscle cells (VSMCs) undergo a transition from contractile to synthetic in response to pro-inflammatory factors around the necrotic core, promoting their migration and macrophage-like transformation ². Currently, the lineage tracing data show that more than 50% of foam cells in atherosclerotic plaque are derived from VSMCs^{3,4}, but the mechanism of VSMC-derived foam cell formation remains unclear.

In fact, endothelial cells (ECs) in the lumen of blood vessel are subjected to a combined stimulation of longitudinal shear stress, circumferential stretch, and radial pressure, whereas VSMCs in the middle layer of the arterial wall are mainly subjected to stretch caused by pressure. Some in vitro studies have demonstrated that stretching can activate a wide range of cellular responses through various mechanoreceptors, such as integrins⁵, ion channels⁶, and piezo ^{6,7}. Oxidative stress is one of the most significant and prevalent cellular responses to mechanical stimuli. As a major pathway for cells to produce ROS, NADPH oxidases (NOX), especially NOX1, 2, and 4, have been frequently reported to be involved in various cellular responses of VSMCs, such as inflammation ⁸⁻¹⁰, proliferation ^{11,12}, migration ¹³⁻¹⁵, and phenotypic transformation ^{11,16}. For more than two decades, numerous studies have shown that activation of a variety of NOXs can induce oxidative stress and LDL oxidation^{8,12,13,17-25}. Some of them were

used to explain the association between hypertension and atherosclerosis. Manea et al. reported that NOX1 and 4 in VSMCs can be regulated by NF- κ B and JAK-STAT signaling pathways, revealing that NOXs are closely related to inflammatory response^{21,26}. Our previous data have also shown that 15% stretching can cause a significant increase in IL-8 expression in both the single-type endothelial cell culture and multiple-type THP-1/EC/VSMC cell culture^{27,28}.

Recently, Swiatlowska et al investigated the effect of static high-pressure condition (180/120 mmHg) on lipid accumulation and transdifferentiation in VSMC using a homemade pressure chamber^{6,29}. Their results showed the static high-pressure condition induced calcium influx through Peizo1 located at the inner and outer membranes of the nucleus to trigger a range of mechanosignaling pathways, such as phospholipid and arachidonic acid signaling and epigenetic regulation. The pulsating blood pressure acting on the wall of the tube is partly converted into stretching, but their pressure device did not convert the static pressure into the stretching on cells. Our group once introduced a microfluidic device to simulate a three-dimensional curved stretch to induce the EC injury and inflammation²⁸. Based on this device, we also further developed a EC-VSMC double cell layer with the adherent THP-1 to induce the foam cell formation under 15% stretch combined with 25 μ g / ml LDL²⁷. However, we found that the lipid accumulation mostly occurred in the adherent THP-1 rather than VSMCs or ECs. This phenomenon may be due to the large ability of the macrophages derived from THP-1 to scavenge ox-LDL.

In general, the stretching of the blood vessel wall caused by blood flow pulsation is less than 7~8%, and more than 10% is considered to be beyond the normal range³⁰⁻³². Based on the susceptibility to atherosclerosis at the bend and bifurcation of blood vessels and the possibility of overstretching of the tube wall in case of blood retention, we speculate that there is a correlation between overstretching of the tube wall and atherosclerosis. Specifically, the formation of VSMC foam cells may be related to overstretching. To test this hypothesis, we used the same microfluidic stretch chips as our previous work and applied a stretch with a total area change rate of 15% to the cultured VSMC alone for 24 h. The obtained results show that 15% stretch causes a significant lipid accumulation in the VSMCs, along with a significant increase in NOX1 and CD36 protein expression. This stretching-induced lipid accumulation can be mitigated by NOX1 inhibitors, as well as antioxidants. Finally, the results also suggest that the increased NOX1 expression caused by 15% stretching is associated with the proven JAK/STAT signaling pathway.

Results

15% stretch causes lipid accumulation in VSMCs

In Figure 1A, a cartoon displays possible atherosclerosis-prone lesions at bend or bifurcation of blood vessels, where the wall of blood vessel may bulge outward due to disturbed blood flow³³. A home-made microfluidic device is used to provide non-uniform, multi-directional, and curved stretching to mimic the stretching profile at the protruding site of the arterial wall. Figure 1B illustrates how a microfluidic device works,

where the amplitude of stretching is the rate of change in the area at the bottom of each cell culture well in the stretched and unstretched conditions. As shown in Figure 1C, the lipid accumulation labeled by Oil Red O (ORO) staining in VSMCs was only significantly increased at 15% stretch and barely changed at 5% stretch compared to no stretch condition. In addition, the addition of 25 $\mu\text{g}/\text{mL}$ LDL to the medium significantly promoted lipid accumulation under all tested conditions. This may be due to the addition of LDL containing some oxidized LDL or partial LDL being oxidized in situ by cell-generated ROS. At the same time, the change in the protein expression of CD36, a scavenger receptor of ox-LDL, is consistent with their corresponding lipid accumulation (Figure 1D). This suggests that the expression of CD36 is sensitive to both the 15% stretch and 25 $\mu\text{g}/\text{mL}$ LDL. However, the expression of two cholesterol efflux transporters, ABCA1 and SR-BI, exhibit no significance between 15% stretch and unstretch condition (Figure S1).

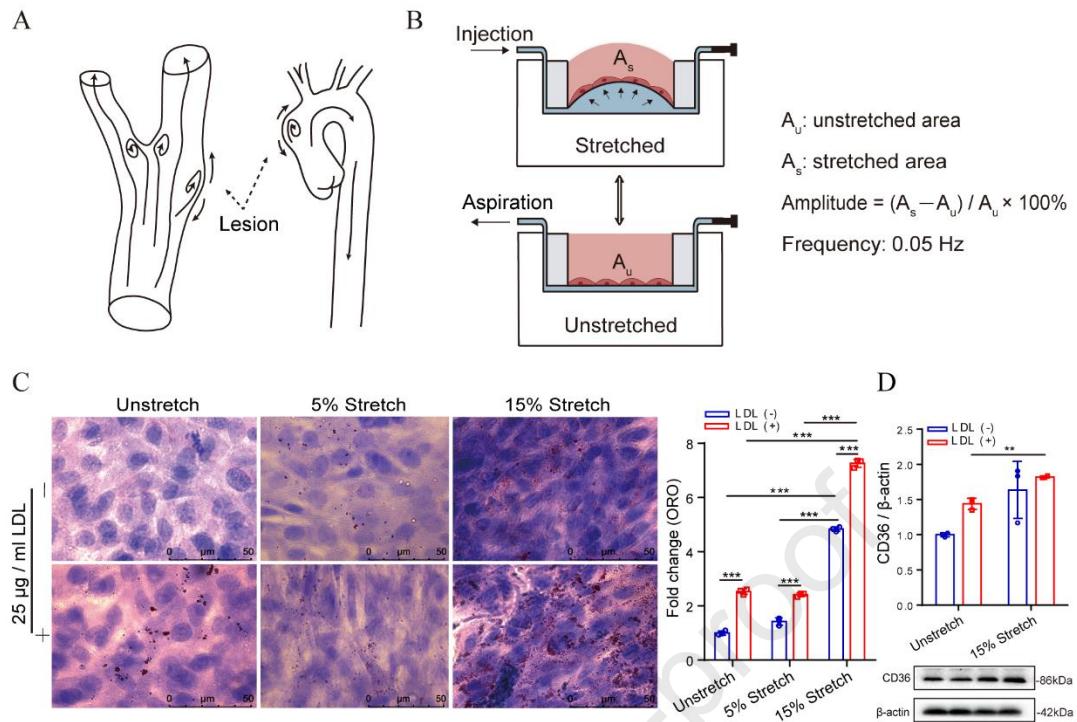


Figure 1. In vitro model of VSMC foam cell formation. (A) Diagram of vascular bulging image; (B) Working principle of the microfluidic chip; (C) Lipid accumulation in T/G HA-VSMCs assessed by Oil Red O staining; (D) Protein expression of CD36 in T/G HA-VSMCs. The data are shown as mean \pm SD ($n = 3$), * $p < 0.05$, ** $p < 0.01$, *** $p < 0.001$, **** $p < 0.0001$, and “ns” indicates no significance.

NOX1 is critical to stretch-induced lipid accumulation

Ox-LDL is one of the key factors in the formation of foam cells and derived from the oxidation of extracellular LDL. It is important to identify the main sources of intracellular ROS for the understand of the lipid accumulation caused by stretching. Since NOXs is one of the main pathways for the production of ROS in cells, we aimed to compare the changes in transcription and protein levels of five NOXs. However, Figure 2A and Figure S2 show that 15% stretching promotes more significant increase

in both NOX1 transcription and protein expression, whereas other investigated NOXs lacked the consistency. Next, intracellular ROS levels were assessed using DCFH, DHE, Deep Red, and MitoSOX probes, and the results in Figure 2B showed that 15% stretching induced a significant increase in ROS levels indicated by these different probes, regardless of identifying as hydrogen peroxide, superoxide anion, or ROS in the cytoplasm or mitochondria. These elevated ROS levels should suggest that more extracellular LDL is oxidized. Furthermore, we selected ML-090, a NOX1-specific inhibitor, and apocynin, a NOX-non-specific inhibitor, and three different ROS scavengers, N-acetyl cysteine (NAC), catalase, and superoxide dismutase (SOD), to validate the role of ROS elimination in the lipid accumulation. As shown in Figure 2C, these reagents except for SOD have a significant inhibitory effect on the lipid accumulation. This suggests that the increase in ROS level associated with NOX1 plays an important role in the VSMC lipid accumulation. According to the SOD failure to reduce the lipid accumulation, we speculate that the extracellular LDL oxidation is mainly due to hydrogen peroxide rather than superoxide anion.

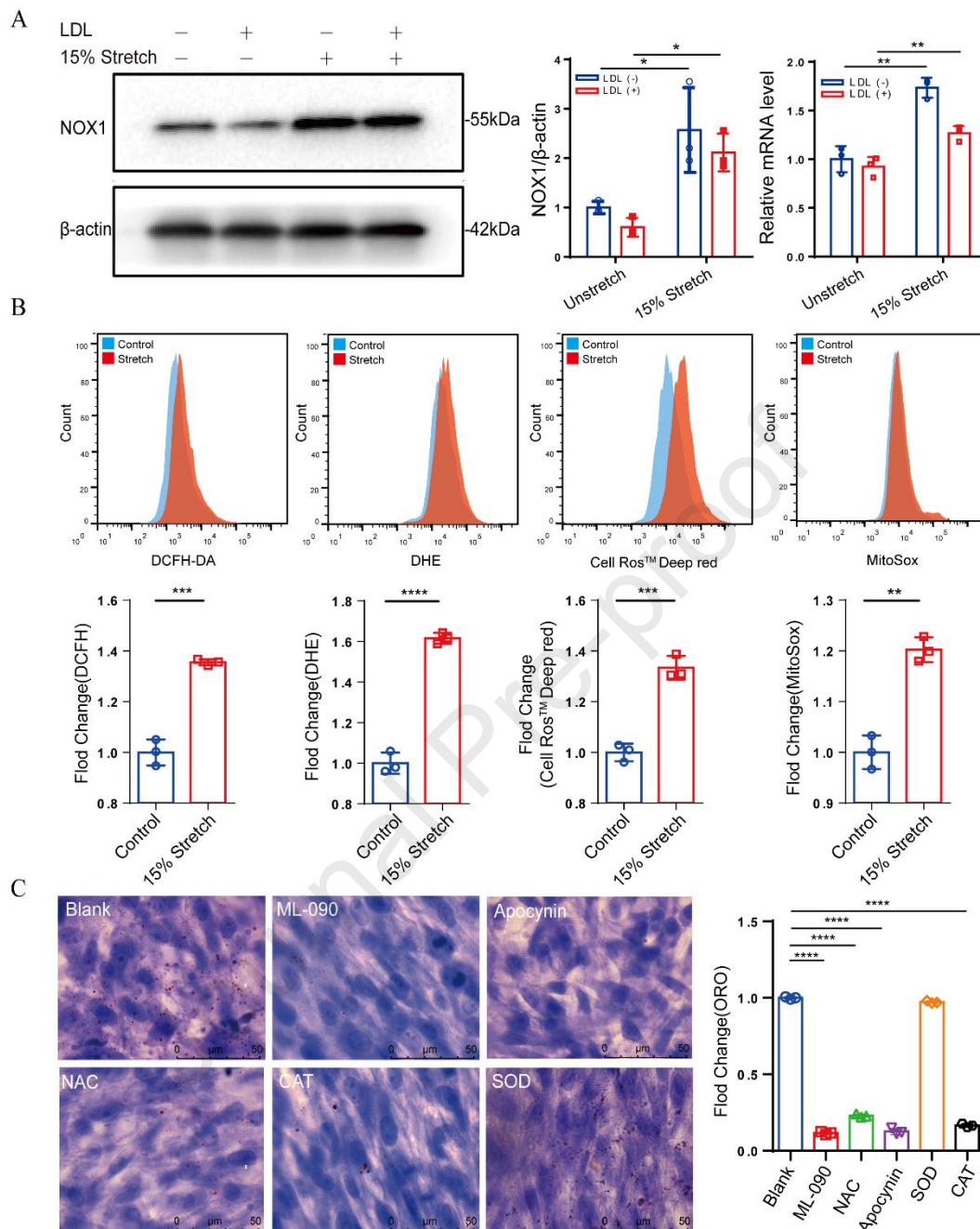


Figure 2: Roles of NOX1 and ROS in the stretch-induced lipid accumulation in VSMCs.

(A) NOX1 transcription and protein expression; (B) ROS level indicated by DCFH, DHE, Deep Red and MitoSOX; (C) Stretch-induced lipid accumulation under different antioxidant treatment, ML-090 (10 μ M), apocynin (300 μ M), NAC (1 mM), catalase (500 IU), SOD (100 IU). The data are shown as mean \pm SD (n = 3), * p < 0.05, ** p <

0.01, *** $p < 0.001$, **** $p < 0.0001$.

Knockdown of NOX1 alleviates stretch-induced lipid accumulation

To evaluate the correlation between NOX1 expression and intracellular ROS level, NOX1 knockdown was performed by constructing a NOX1-deficient VSMC line using a lentiviral GFP vector (Figure 3A). The NOX1 knockdown significantly reduced both the lipid accumulation and BODIPY-labeled intracellular lipid oxidation in the presence of 15% stretch (Figure 3B and C). The results of Figure 3D and E show that NOX1 knockdown also significantly inhibited the stretch-induced ROS production indicated either DCFH or DHE. However, the change in DCFH-labeled ROS level is much more pronounced than the DHE indicated change, suggesting that LDL oxidation is more dependent on hydrogen peroxide than superoxide anion. This is consistent with the results that SOD treatment did not alleviate lipid accumulation caused by stretching. As a result, these data demonstrate that NOX1 plays a key role in the stretch-induced lipid accumulation.

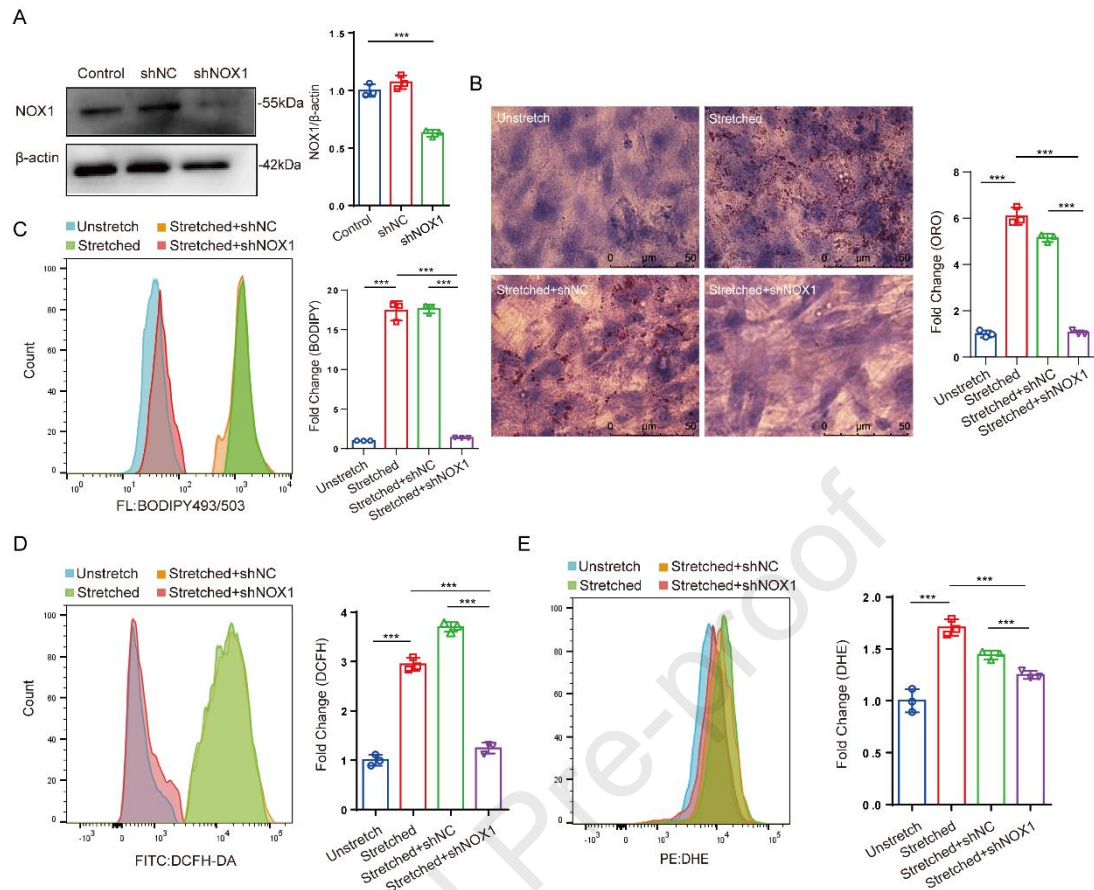


Figure 3: NOX1 knockdown reduces the stretch-induced lipid accumulation and ROS level in VSMCs. (A) Verification of NOX1 knockdown; (B and C) Lipid accumulation and lipid oxidation indicated by ORO and BODIPY, respectively; (D and E) ROS level indicated by DCFH and DHE. The data are shown as mean \pm SD (n = 3), *p < 0.05, **p < 0.01, ***p < 0.001, ****p < 0.0001.

15% stretch induces NOX1 upregulation via JAK/STAT signaling pathway

It has been reported that the JAK/STAT signaling pathway regulates the expression of NOX1 in VSMC²², so we examined several key factors of this signaling pathway. As shown in Figures 4A and B, 15% stretching induced the phosphorylation of STAT1 and STAT3, as well as the expression of IL-6 and IFN- γ . In contrast, the addition of LDL has

no significant effect on this signaling pathway. On the other hand, we used stattic, a STAT3 phosphorylation inhibitor, to further confirm whether this pathway is involved in the regulation of NOX1 expression and lipid accumulation. As shown in Figure 4C-E, stattic significantly inhibited NOX1 expression, lipid oxidation, and lipid accumulation. Therefore, the JAK/STAT signaling pathway can be targeted to inhibit NOX1 expression and lipid accumulation in VSMCs.

Journal Pre-proof

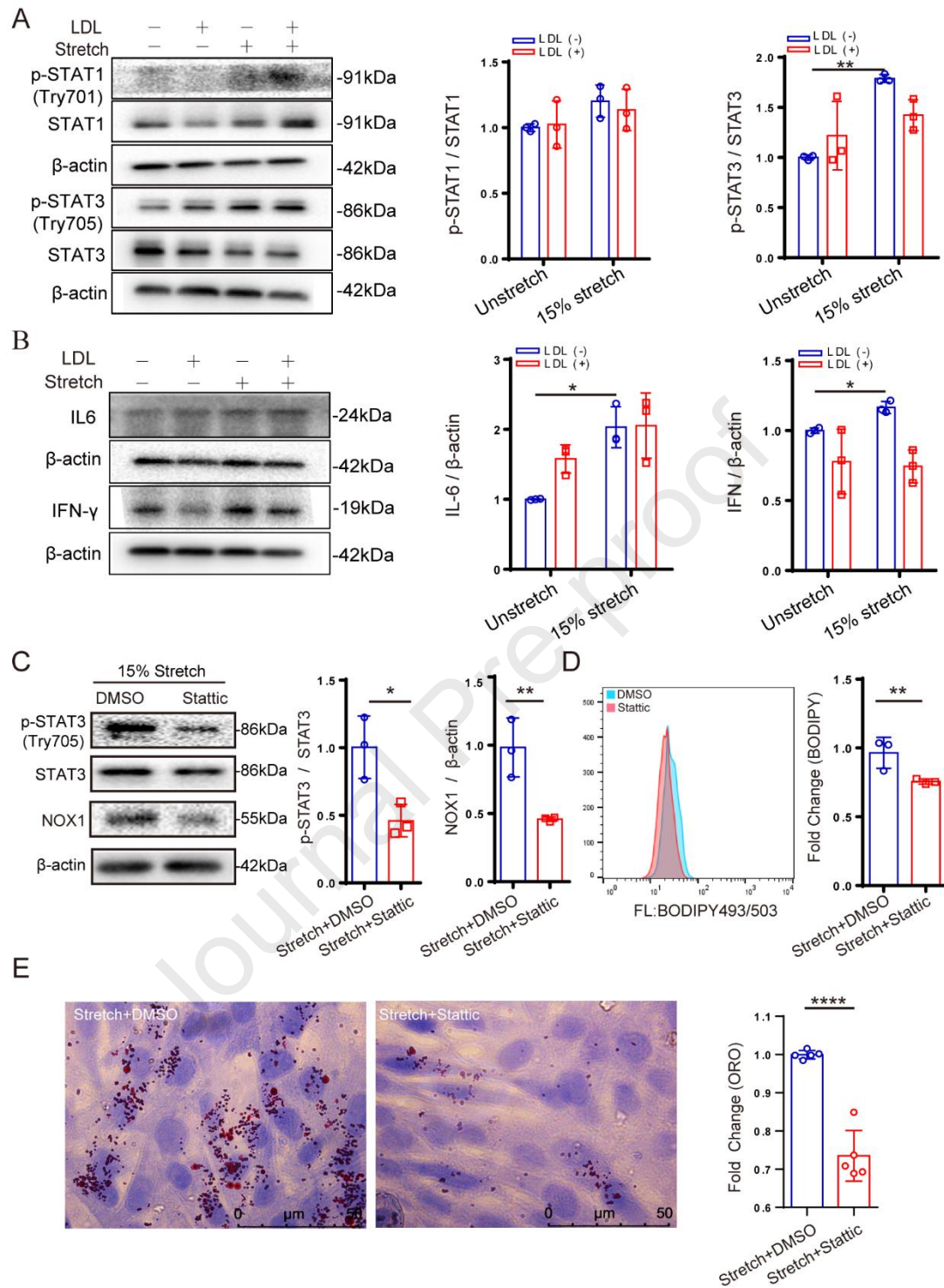


Figure 4: Stretch-induced lipid accumulation depends on the JAK/STAT signaling pathway. (A and B) 15% stretch promotes the STAT1/3 phosphorylation and the expression of IL-6 and IFN- γ . (C-E) Inhibition of STAT3 phosphorylation and NOX1

expression, lipid oxidation, and lipid accumulation under 50 μ M static treatment.

The data are shown as mean \pm SD ($n = 3$), * $p < 0.05$, ** $p < 0.01$, *** $p < 0.001$, **** $p < 0.0001$.

Discussion

Atherosclerotic plaque formation at arterial bends and bifurcations is closely associated with hemodynamic disturbances, where localized overstretching of the vascular wall may serve as a critical biomechanical trigger. While macrophage-derived foam cells have long been the focus of atherosclerosis research, emerging evidence highlights that VSMC contribute substantially to plaque foam cell populations^{2,3}. This study elucidates a novel mechanism by which pathological overstretch (15%) directly induces lipid accumulation in VSMCs via NOX1-dependent oxidative stress, mediated through the JAK/STAT3 signaling pathway. These findings advance our understanding of VSMC-driven atherogenesis under biomechanical stress.

Our microfluidic model, which simulates non-uniform, multidirectional stretch mimicking vascular bulging, revealed that 15% cyclic stretch significantly upregulated NOX1 expression and intracellular ROS levels in VSMCs (Figure 2A and B). This ROS surge correlated with enhanced lipid accumulation, likely driven by the oxidation of native LDL in the microenvironment, as evidenced by the marked increase in CD36—a scavenger receptor for oxidized LDL (Figure 1D). Notably, lipid accumulation was attenuated by NOX1 inhibition (ML-090), ROS scavengers (NAC, catalase), and NOX1 knockdown, underscoring NOX1 as a central mediator of stretch-induced oxidative

stress(Figure 2C and 3). The inefficacy of SOD further suggests that hydrogen peroxide, rather than superoxide anion, predominantly mediates LDL oxidation in this context(Figure 2C). These observations align with prior studies linking NOX1 to VSMC inflammation and phenotypic switching, yet uniquely identify its role in mechanotransduction-driven lipid accumulation. A key distinction of this work lies in the use of a VSMC monoculture system, which isolates the direct effects of stretch on VSMCs without confounding interactions with macrophages or endothelial cells. This approach revealed that dedifferentiated VSMCs, with inherently higher NOX1 and CD36 expression, are particularly susceptible to stretch-induced lipid accumulation. Such phenotypic plasticity underscores the heterogeneity of VSMCs in atherosclerosis and their capacity to adopt pro-atherogenic traits under mechanical stress. However, the reliance on a cell line rather than primary VSMCs warrants caution, as in vivo VSMCs may exhibit divergent responses influenced by their microenvironment.

Mechanistically, the JAK/STAT3 pathway emerged as a critical regulator of NOX1 expression under overstretch. Phosphorylation of STAT1/3 and elevated IL-6/IFN- γ levels indicate that mechanical stress activates inflammatory signaling, which in turn upregulates NOX1(Figure 4A and B). The suppression of NOX1 and lipid accumulation by STAT3 inhibition (stattic) solidifies this pathway's involvement(Figure 4C). This aligns with reports that inflammatory cytokines like IFN- γ regulate NOX1 via JAK/STAT in VSMCs, but extends these findings to a biomechanical context. Importantly, our model highlights a feedforward loop: overstretch-induced endothelial damage may recruit inflammatory cells, releasing cytokines that amplify NOX1 expression in neighboring

VSMCs, thereby exacerbating lipid retention and plaque progression.

Clinically, these findings underscore NOX1 as a potential therapeutic target to mitigate VSMC foam cell formation in high-risk vascular regions prone to overstretch. The efficacy of antioxidants and NOX1 inhibitors in our model supports further exploration of these agents in preclinical studies. Moreover, the identification of JAK/STAT3 as an upstream regulator opens avenues for repurposing existing anti-inflammatory therapies to disrupt mechanosensitive pathways in atherosclerosis.

Conclusions

In conclusion, this study establishes a direct link between pathological overstretch and VSMC foam cell formation, mediated via NOX1-driven oxidative stress and JAK/STAT3 activation. These insights not only deepen our understanding of biomechanical contributions to atherosclerosis but also highlight novel targets for intervention in vascular regions susceptible to hemodynamic stress.

Methods

Reagents and antibodies

Dulbecco's Modified Eagle Medium (DMEM) and fetal bovine serum (FBS) were obtained from Gibco (Thermo Fisher Scientific). Human LDL was obtained from Yiyuan Biotechnologies (Beijing, China). Oil red O powder was obtained from Biolabs (Beijing, China). Antibodies against NOX1 (1:2000, CSB-PA443876), NOX3 (1:2000, CSB-PA015960ESR2HU), and DUOX2 (1:2000, CSB-PA007229ESR1HU) were obtained from

Cusabio (Wuhan, China). Antibodies against NOX2 (1:5000, ab129068), NOX4 (1:2000, ab109225), SR-B1 (1:1000, ab53629), ABCA1 (1:1000, ab18180) and IFN- γ (1:1000, ab133566) were from Abcam. Antibodies against CD36 (1:1000, 18836-1-AP), DUOX1 (1:2000, 67226-1-Ig) and IL-6 (1:600, 26404-1-AP) were from Proteintech. Antibodies against JAK2 (1:1000, 3230T), phospho-JAK2 (Tyr1007) (1:1000, 4406T), Stat1 (1:1000, 9172T), phospho-Stat1 (Tyr701) (1:1000, 7649T), Stat3 (1:1000, 9139T), phospho-Stat3 (Tyr705) (1:2000, 9145T), stattic (97598), and protease/phosphatase inhibitor cocktail (100x, 5872S) were obtained from Cell Signaling Technology. Antibody against β -actin (1:10000, 109444-T32) was obtained from Sino Biological (Beijing, China). RNAprep Pure Micro Kit was obtained from Tiangen (Beijing, China). TransScript First-Strand cDNA Synthesis SuperMix was obtained from TransGen Biotech (Beijing, China). 2', 7'-Dichlorodihydrofluorescein diacetate (DCFH-DA) was purchased from Sigma-Aldrich. Dihydroethidium (DHE) was purchased from ApexBio. Cell Ros™ Deep Red and MitoSOX™ Red Mitochondrial Superoxide Indicator was purchased from (Invitrogen). ML-090 (NOX1 inhibitor, 15172) and apocynin (NOXs inhibitor, 119761) were obtained from Cayman Chemical (Ann Arbor, MI, USA). N-acetyl cysteine (NAC), and Catalase was obtained from Yuanye Biotechnologies (Shanghai, China). Superoxide dismutase (SOD) was obtained from Beyotime (Shanghai, China).

Microfluidic stretching device

The microfluidic stretching device used consists of three layers of polydimethylsiloxane (PDMS), an upper layer with array cell culture pores, a middle layer with stretchable deformation, and a lower layer with microfluidic fluid grooves. The working principle

and stretch features are described in detail in our previous work^{27,28}. Briefly, one side of the microfluidic channel is blocked, while another side is connected to a syringe pump. After injecting a certain volume of water into the chamber just below the cell culture well, the middle layer membrane is deformed upwards to form a spherical cap, transducing stretch stimulus to attached cells. The amplitude is determined by the volume of injected water and the frequency is determined by the injection and aspiration duration. One cycle takes 20 seconds (0.05 Hz).

Cell culture

An aortic VSMC line (T/G HA-VSMC) is maintained by our laboratory and a human aortic smooth muscle cells (HUM-iCell-c010, primary) were purchased from Cell Technology Co., Ltd (Shanghai, China). Cells were cultured in DMEM containing 10% FBS at 37 °C in a 5% CO₂ incubator. 50 µl of cell suspension (1 x 10⁵ cells/ml) was added into each well (6-mm diameter) coated with fibronectin. When the cells reached over 90% confluence, the medium was replaced with fresh complete medium with or without the addition of 25 µg / ml LDL. Next, the syringe pump started to run with a program-controlled volume of liquid injection and aspiration, providing the desired stretch (15%, 0.05 Hz), while the cells were cultured in non-stretched device as the control.

Oil red O staining

After stretched for 24 h, the cells in each well were fixed with 4% (m/v) paraformaldehyde in a phosphate-buffered saline (PBS) for 30 min, and then stained with 2.4% (m/v) oil red O staining solution (Biolabs, Shanghai, China) for 1 h. The

stained cells were incubated with 60% (v/v) isopropanol solution for 15 second and followed by a hematoxylin solution (Biodragon Immunotechnologies, Beijing, China) for 3 min. Then, the hematoxylin solution was discarded and the cells were washed with tap water for 2-3 times. The cell-fixed membrane was cut off and mounted on a slide for observation. Images were acquired with a microscope (DM6B, Leica Microsystems) and the amount of the red lipid droplets was counted by Image J software (Wayne Rasband, NIH, USA).

Western blotting

After VSMCs in the wells were treated with the indicated conditions for 24 h, the cell lysates were prepared using RIPA buffer (Beyotime, Shanghai, China) with protease/phosphatase inhibitor phenylmethylsulfonyl (PMSF), and the protein concentration was quantified using NanoDrop One (Thermo Scientific). The proteins were separated by 8.5% SDS-PAGE, and then electrically transferred into a polyvinylidene difluoride (PVDF) membrane. Subsequently, the membranes were immersed in 5% non-fat milk in Tris-buffered saline with Tween (TBST) at room temperature for 1 h with shaking. After that, the membranes were incubated with the indicated primary antibodies at 4 °C for overnight, following by incubation horseradish peroxidase (HRP)-labeled goat anti-rabbit or anti-mouse antibodies for 1 h at room temperature. The immunobands were visualized using an enhanced chemiluminescence (EMD, Millipore Corp., Burlington, MA, USA) and quantified by using an imaging system (Image Lab, Bio-Rad Laboratories).

qPCR

After treatment, the total RNA was isolated using RNAPrep Pure Cell Kit (Tiangen, Beijing, China) according to the manufacturer's introduction. Single-strand cDNA was synthesized from 1 μ g of total RNA using TransScript First-Strand cDNA Synthesis SuperMix (TransGen Biotech, Beijing, China). Quantitative analysis of NOX1-5, DUOX1, DUOX2, and GAPDH mRNA were carried out on Max3000P Real-time PCR instrument (Agilent, La Jolla, CA, USA) using TransStart Top Green qPCR SuperMix (+Dye II) (TransGen Biotech, Beijing, China). The primer sequences for target gene were as follows: *NOX1* (forward 5'-CTGCTTCCTGTGTGTCGCAA-3' and reverse 5'-AGGCAGATCATATAGGCCACC-3'), *NOX2* (forward 5'-GTGCGTGCTGCTCAACAAGAGTT-3' and reverse 5'-ATGGTGTGAATCGCAGAGTGAAGTG-3'), *NOX3* (forward 5'-CGGATTGTT CGAGGCCAAAC-3' and reverse 5'-GCCAGAAAATTGAGGCACGG-3'), *NOX4* (forward 5'-AGCAGAGCCTCAGCATCTGTTCTT-3' and reverse 5'-TGGTTCTCCTGCTTGGAACCTTCT-3'), *NOX5* (forward 5'-CTGCTGGTGCCTGGAATCTTGTT-3' and reverse 5'-GCCGCTTGATGAGGAGATGAGTGA-3'), *DUOX1* (forward 5'-CGTGAGCACCCAAGCCTACAAAGT-3' and reverse 5'-TCCCGCACATCTTCAACCAACACAT-3'), *DUOX2* (forward 5'-AGGATACCGTCCTTTCCTAGAC-3' and reverse 5'-GGTTCTCCCGAATCCAGTAGTT-3'), *GAPDH* (forward 5'-ACATCAAGAAGGTGGTGAAGCAGGC-3' and reverse 5'-GGTGTGCTGTTGAAGTCAGAGGAG-3'). The mRNA level of each target gene was normalized to *GAPDH* and analyzed using the $2^{-\Delta\Delta C_t}$ method.

ROS assays

After treated with the indicated conditions, the cells were washed twice with PBS.

Subsequently, 50 μ L of serum-free medium with 5 μ M DCFH-DA, DHE, and Deep Red, MitoSOX was added into each cell culture well the incubation at 37°C or 30 min. After that, the cells were collected in desired volume of PBS for flow cytometry (FACS Aria III, Brand, USA) or microplate reader (BioTek, VT, USA) for measurement.

NOX1 knockdown

shRNAs for NOX1 constructs in lentiviral GFP vector (pLKO.1) were purchased from Tsingke Technologies (Beijing, China). In brief, HEK293T cells were transfected with either empty vector or target gene constructs with psPAX.2 and pMD2.G second-generation lentiviral packaging system. After 48 h incubation, the lentivirus particles in the medium were collected and filtered to infect the VSMC. After 48 h infection, 2 μ g / ml puromycin was added into the cell culture medium to obtain the stable cell lines with successful transduction. The following sequences, inserted into an empty pLKO.1-TRC vector, were used for short hairpin RNA (shRNA) knockdowns:

shScramble:

CCGGGAAGGCCTGAAGGTCAGATACCTCGAGGTATCTGACCTTCAGGCCTTCTTTTTT

NOX1-shRNA1:

CCGGGCCTATATGATCTGCCTACATCTCGAGATGTAGGCAGATCATATAGGCTTTTTT.

NOX1-shRNA2:

CCGGCCGCACACTGAGAAAGCAATTCTCGAGAATTGCTTTCTCAGTGTGCGGTTTTTT.

NOX1-shRNA3:

CCGGCCAAGGTTGTTATGCACCCATCTCGAGATGGGTGCATAACAACCTTGGTTTTTTT.

NOX1-shRNA4:

CCGGGAACAGGAGATGGAGGAATTACTCGAGTAATTCCTCCATCTCCTGTTCTTTTTT.

BODIPY staining

The cells in the each well were rinsed with PBS three times and incubated in 2 μ M 4,4-difluoro-1,3,5,7,8-pentamethyl-4-bora-3a,4a-diaza-s-indacene (BODIPY 493/503, Cayman Chemical) staining solution in the dark for 15 min at 37 °C, following by washing with PBS. The cells were trypsinized and centrifuged with 250 g for 5 min at 4°C. After that, the supernatant was aspirated carefully and the cells were resuspended in 500 μ l PBS. Flow cytometry was used for quantification at 488 nm / 525 nm.

Statistical analysis

The data are expressed as the means \pm SD. Comparisons between two groups were performed using the unpaired Student's t-test, and comparisons among three or more groups were performed using one-way or two-way analysis of variance (ANOVA) followed by Bonferroni's multiple comparison test. P values < 0.05 were considered statistically significant. All statistical analyses were performed with GraphPad Prism 6.01.

Data availability

The datasets used and/or analysed during the current study available from the corresponding author on reasonable request.

References

- 1 Mahmoudi, M., Curzen, N. & Gallagher, P. J. Atherogenesis: the role of inflammation and infection. *Histopathology* **50**, 535-546, doi:10.1111/j.1365-2559.2006.02503.x (2007).
- 2 Liu, Y. X., Yuan, P. Z., Wu, J. H. & Hu, B. Lipid accumulation and novel insight into vascular smooth muscle cells in atherosclerosis. *J Mol Med (Berl)* **99**, 1511-1526, doi:10.1007/s00109-021-02109-8 (2021).
- 3 Allahverdian, S., Chehroudi, A. C., McManus, B. M., Abraham, T. & Francis, G. A. Contribution of intimal smooth muscle cells to cholesterol accumulation and macrophage-like cells in human atherosclerosis. *Circulation* **129**, 1551-1559, doi:10.1161/CIRCULATIONAHA.113.005015 (2014).
- 4 Allahverdian, S. & Francis, G. A. Cholesterol homeostasis and high-density lipoprotein formation in arterial smooth muscle cells. *Trends Cardiovasc Med* **20**, 96-102, doi:10.1016/j.tcm.2010.09.002 (2010).
- 5 Kappert, K. *et al.* Integrins alphavbeta3 and alphavbeta5 mediate VSMC migration and are elevated during neointima formation in the rat aorta. *Basic Res Cardiol* **96**, 42-49, doi:10.1007/s003950170076 (2001).
- 6 Swiatlowska, P. *et al.* Hypertensive Pressure Mechanosensing Alone Triggers Lipid Droplet Accumulation and Transdifferentiation of Vascular Smooth Muscle Cells to Foam Cells. *Adv Sci (Weinh)* **11**, e2308686, doi:10.1002/advs.202308686 (2024).
- 7 Barbeau, S. *et al.* [Involvement of the Piezo1 and TRPV4 stretch-activated channels in pulmonary hypertension]. *Rev Mal Respir* **39**, 79-83, doi:10.1016/j.rmr.2022.01.013 (2022).
- 8 Lamb, F. S., Choi, H., Miller, M. R. & Stark, R. J. Vascular Inflammation and Smooth Muscle Contractility: The Role of Nox1-Derived Superoxide and LRRC8 Anion Channels. *Hypertension* **81**, 752-763, doi:10.1161/HYPERTENSIONAHA.123.19434 (2024).
- 9 Panthiya, L., Tocharus, J., Chaichompoo, W., Suksamrarn, A. & Tocharus, C. Hexahydrocurcumin mitigates angiotensin II-induced proliferation, migration, and inflammation in vascular smooth muscle cells. *EXCLI J* **22**, 466-481, doi:10.17179/excli2023-6124 (2023).
- 10 Wu, J. H. *et al.* Drebrin attenuates atherosclerosis by limiting smooth muscle cell transdifferentiation. *Cardiovasc Res* **118**, 772-784, doi:10.1093/cvr/cvab156 (2022).
- 11 Vendrov, A. E. *et al.* NOXA1-dependent NADPH oxidase regulates redox signaling and phenotype of vascular smooth muscle cell during atherogenesis. *Redox Biol* **21**, 101063, doi:10.1016/j.redox.2018.11.021 (2019).
- 12 Ping, S. *et al.* Protein disulfide isomerase-mediated apoptosis and proliferation of vascular smooth muscle cells induced by mechanical stress and advanced glycosylation end products result in diabetic mouse vein graft atherosclerosis. *Cell Death Dis* **8**, e2818, doi:10.1038/cddis.2017.213 (2017).
- 13 Jagadeesha, D. K., Takapoo, M., Banfi, B., Bhalla, R. C. & Miller, F. J., Jr. Nox1 transactivation of epidermal growth factor receptor promotes N-cadherin shedding and smooth muscle cell migration. *Cardiovasc Res* **93**, 406-413, doi:10.1093/cvr/cvr308 (2012).
- 14 Duan, H. *et al.* MicroRNA-217 suppresses homocysteine-induced proliferation and migration of vascular smooth muscle cells via N-methyl-D-aspartic acid receptor inhibition. *Clin Exp Pharmacol Physiol* **43**, 967-975, doi:10.1111/1440-1681.12611 (2016).
- 15 Kim, J. *et al.* The flagellin-TLR5-Nox4 axis promotes the migration of smooth muscle cells in atherosclerosis. *Exp Mol Med* **51**, 1-13, doi:10.1038/s12276-019-0275-6 (2019).
- 16 Starke, R. M. *et al.* Cigarette Smoke Initiates Oxidative Stress-Induced Cellular Phenotypic

- Modulation Leading to Cerebral Aneurysm Pathogenesis. *Arterioscler Thromb Vasc Biol* **38**, 610-621, doi:10.1161/ATVBAHA.117.310478 (2018).
- 17 Dikalov, S. I. *et al.* Distinct roles of Nox1 and Nox4 in basal and angiotensin II-stimulated superoxide and hydrogen peroxide production. *Free Radic Biol Med* **45**, 1340-1351, doi:10.1016/j.freeradbiomed.2008.08.013 (2008).
- 18 Hanna, I. R., Taniyama, Y., Szocs, K., Rocic, P. & Griendling, K. K. NAD(P)H oxidase-derived reactive oxygen species as mediators of angiotensin II signaling. *Antioxid Redox Signal* **4**, 899-914, doi:10.1089/152308602762197443 (2002).
- 19 Inoue, N. *et al.* Stretch force on vascular smooth muscle cells enhances oxidation of LDL via superoxide production. *Am J Physiol* **274**, H1928-1932, doi:10.1152/ajpheart.1998.274.6.H1928 (1998).
- 20 Sima, A. V. *et al.* Effect of irreversibly glycosylated LDL in human vascular smooth muscle cells: lipid loading, oxidative and inflammatory stress. *J Cell Mol Med* **14**, 2790-2802, doi:10.1111/j.1582-4934.2009.00933.x (2010).
- 21 Manea, A., Tanase, L. I., Raicu, M. & Simionescu, M. Jak/STAT signaling pathway regulates nox1 and nox4-based NADPH oxidase in human aortic smooth muscle cells. *Arterioscler Thromb Vasc Biol* **30**, 105-112, doi:10.1161/ATVBAHA.109.193896 (2010).
- 22 La Manna, S. *et al.* Antioxidant Effects of PS5, a Peptidomimetic of Suppressor of Cytokine Signaling 1, in Experimental Atherosclerosis. *Antioxidants (Basel)* **9**, doi:10.3390/antiox9080754 (2020).
- 23 Schiffrin, E. L. & Canadian Institutes of Health Research Multidisciplinary Research Group on, H. Beyond blood pressure: the endothelium and atherosclerosis progression. *Am J Hypertens* **15**, 115S-122S, doi:10.1016/s0895-7061(02)03006-6 (2002).
- 24 Yokoyama, M., Inoue, N. & Kawashima, S. Role of the vascular NADH/NADPH oxidase system in atherosclerosis. *Ann N Y Acad Sci* **902**, 241-247; discussion 247-248, doi:10.1111/j.1749-6632.2000.tb06319.x (2000).
- 25 Sorescu, D. *et al.* Superoxide production and expression of nox family proteins in human atherosclerosis. *Circulation* **105**, 1429-1435, doi:10.1161/01.cir.0000012917.74432.66 (2002).
- 26 Manea, A., Tanase, L. I., Raicu, M. & Simionescu, M. Transcriptional regulation of NADPH oxidase isoforms, Nox1 and Nox4, by nuclear factor-kappaB in human aortic smooth muscle cells. *Biochem Biophys Res Commun* **396**, 901-907, doi:10.1016/j.bbrc.2010.05.019 (2010).
- 27 Gu, X., Xie, S., Hong, D. & Ding, Y. An in vitro model of foam cell formation induced by a stretchable microfluidic device. *Sci Rep* **9**, 7461, doi:10.1038/s41598-019-43902-3 (2019).
- 28 Wang, J., Fan, B., Wei, Y., Suo, X. & Ding, Y. A simple multi-well stretching device to induce inflammatory responses of vascular endothelial cells. *Lab Chip* **16**, 360-367, doi:10.1039/c5lc01416f (2016).
- 29 Swiatlowska, P. *et al.* Pressure and stiffness sensing together regulate vascular smooth muscle cell phenotype switching. *Sci Adv* **8**, eabm3471, doi:10.1126/sciadv.abm3471 (2022).
- 30 Wang, L. *et al.* Secreted miR-27a Induced by Cyclic Stretch Modulates the Proliferation of Endothelial Cells in Hypertension via GRK6. *Sci Rep* **7**, 41058, doi:10.1038/srep41058 (2017).
- 31 Mantella, L. E. *et al.* Fingerprint of long non-coding RNA regulated by cyclic mechanical stretch in human aortic smooth muscle cells: implications for hypertension. *Mol Cell Biochem* **435**, 163-173, doi:10.1007/s11010-017-3065-2 (2017).
- 32 Paravicini, T. M., Montezano, A. C., Yusuf, H. & Touyz, R. M. Activation of vascular p38MAPK by

mechanical stretch is independent of c-Src and NADPH oxidase: influence of hypertension and angiotensin II. *J Am Soc Hypertens* **6**, 169-178, doi:10.1016/j.jash.2012.01.002 (2012).

- 33 Wang, X. & Ge, J. Haemodynamics of atherosclerosis: a matter of higher hydrostatic pressure or lower shear stress? *Cardiovasc Res* **117**, e57-e59, doi:10.1093/cvr/cvab001 (2021).

Acknowledgements

This project was supported by the National Natural Science Foundation of China (31571481, 31771585, and 32070799).

Author Contributions

Zhang and Li successively carried out the experimental work, Ding (SQ) and Xu participated in the additional experiments, Su and Cui provided technical assistance, and Ding (YS) designed the experiment and wrote the manuscript.

Competing Interests

The authors declare no competing interests.

Ethical approval

This study does not contain any studies with human or animal subjects performed by any of the authors.

Journal Pre-proof

Declaration of competing interest

The authors declare that there are no financial interests/personal relationships that could be considered as potential competing interests that would affect the work reported in this paper.

Journal Pre-proof